Quantum Electronics **48** (7) 637–640 (2018)

https://doi.org/10.1070/QEL16621

Formation of core–shell Fe@Al nanoparticles by laser irradiation of a mixture of colloids in ethanol

E.V. Barmina, G.A. Shafeev

Abstract. **The formation of Fe@Al nanoparticles, containing an iron core and an aluminium shell, under laser irradiation of a mixture of individual colloids of nanoparticle components in absolute ethanol has experimentally been investigated for the first time. A mixture of colloids was irradiated by a sequence of neodymium laser pulses with duration of 10 ns and repetition rate of 10 kHz. It is found that the size of the iron core of core–shell nanoparticles increases from the initial value of 8 nm to 20 nm under irradiation, whereas the aluminium shell size decreases from the initial value of 120 nm to 70 nm. The formation of core–shell nanoparticles is explained by the difference in the melting temperatures of the initial nanoparticles and the difference in the lattice parameters of their materials. The thus obtained core–shell nanoparticles retain ferromagnetic properties. Possible applications of these nanoparticles are discussed.**

Keywords: *laser irradiation, liquid, core–shell nanoparticles.*

1. Introduction

Laser ablation of solids is one of the ways to fabricate nanoparticles, which is alternative to chemical and other methods. The synthesis of chemically pure and biocompatible nanoparticles is an actual problem of modern science, because the range of application of nanoparticles in medicine and in biology is constantly expanding [1, 2]. These particles can be formed using laser ablation of solids in liquids [3]. In contrast to the chemical processes of nanoparticle formation, stabilising ions and surfactants are absent in the synthesised colloids during laser ablation. In addition, the newly formed nanoparticles remain in the same liquid where a solid target was ablated; hence, they can interact with the laser beam. Generally, this interaction changes the size distribution function of nanoparticles. For example, laser irradiation of an ensemble of nanoparticles in a liquid causes their fragmentation: the average nanoparticle size decreases, and the second maximum arises in their distribution function in the range of smaller sizes. If a mixture of nanoparticles of different materials is irradiated, one can observe, simultaneously with fragmentation, alloying of nanoparticles (provided that the nanoparticles of the mixture have close melting temperatures). For example, laser irradiation of gold and silver leads to the formation of nanoparticles of an Au–Ag alloy, in which the ratio of metals is determined by their total amount in the initial mixture of colloids [4, 5]. The reason is that Au and Ag are mixed in any proportions, because these metals have close lattice parameters.

Fragmentation of nanoparticles under laser irradiation is not the only scenario: short (picoseconds) laser pulses may cause agglomeration of Au and Ag nanoparticles [6, 7]. Agglomeration of Au nanoparticles is also observed under laser irradiation of colloids in liquids containing β-active additives, e.g., tritium [8]. In both cases, the agglomeration is explained by the excess charge of nanoparticles.

If the melting temperatures of nanoparticles forming a mixture significantly differ, laser irradiation of this mixture may lead to the formation of core–shell nanoparticles. This process is determined by the difference in the crystallisation temperatures of nanoparticles cooled after the laser pulse. Upon cooling, nanoparticles with a higher melting temperature become solid earlier than those with a lower melting temperature. As a result, a nanoparticle that is still liquid envelopes a more refractory (which already turned to solid) nanoparticle to form a shell around it. These core–shell nanoparticles were obtained under laser irradiation of mixtures of Al and Ti nanoparticles and mixtures of Al nanoparticles and Co nanorods [9, 10]. Aluminium, which has a lower (650 °C) melting temperature than Ti and Co, forms shells around more refractory cores in both cases. Due to the deviation of laser heating from equilibrium, these nanoparticles can be formed even when there are stable homogeneous phases of the corresponding alloy. Apparently, a metal alloy cannot arise in this case, because the solidification time of particles is short in comparison with their interdiffusion time.

In [9, 10], the sizes of nanoparticles forming core–shell nanoobjects as a result of laser irradiation were comparable. It is of interest to consider the case where the sizes of nanoparticles forming a shell greatly exceed the sizes of core nanoparticles. In this paper, we report the results of an experimental study of the formation of core–shell nanoparticles with a small (~10 nm) size of iron core and a relatively large (~100 nm) diameter of aluminium shell.

2. Experimental

We used a mixture of iron and aluminium nanoparticles in absolute ethanol. Note that nanoparticles of both types were obtained by methods different from laser ablation in liquids: aluminium nanoparticles were synthesised as a result of elec-

E.V. Barmina A.M. Prokhorov General Physics Institute, Russian Academy of Sciences, ul. Vavilova 38, 119991 Moscow, Russia; e-mail: barminaev@gmail.com;
G.A. Shafeev A.M. Prokhorov General Physics Institute, Russian Academy of Sciences, ul. Vavilova 38, 119991 Moscow, Russia; National Research Nuclear University 'MEPhI', Kashirskoe sh. 31, 115409 Moscow, Russia

Received 2 February 2018; revision received 16 April 2018
Kvantovaya Elektronika **48** (7) 637–640 (2018)
Translated by Yu.P. Sin'kov

tric explosion of fine Al wires in vacuum [Alex (aluminium explosion) nanoparticles], while iron nanoparticles by obtained chemically: by reducing an iron salt in polyol at an elevated temperature [11]. In contrast to the previous investigations on laser alloying of nanoparticles in liquids [9, 10], our objects of study were nanoparticles with sizes differing by almost an order of magnitude. Iron nanoparticles are ~8 nm in size, and some of them exhibit faceting, whereas aluminium nanoparticles have a size of ~100 nm, and they often have a hexagonal shape. In addition, the sample contains also chains of nanoparticles, consisting of two, three, or more interalloyed small particles. The suspension was irradiated by 1064-nm neodymium laser pulses with an FWHM of 10 ns, a repetition frequency of 10 kHz, and energy of ~1 mJ. The laser beam was focused in the liquid by a lens with a focal length of 3 cm. The laser power density (beam intensity in the waist) in the suspension was estimated to be 10^{10} W cm^{-2}. It is rather difficult to obtain a more accurate value, because one must take into account the beam focusing conditions in the liquid and the radiation absorption and scattering by the suspension. The morphology of nanoparticles and their size distribution were determined from transmission electron microscopy (TEM) images of the samples. Extinction spectra of nanoparticles were recorded on an Ocean Optics fibre-optic spectrometer.

3. Results and discussion

TEM images of the initial mixture of nanoparticles are shown in Fig. 1. The average sizes of iron and aluminium nanoparticles are, respectively, 8 and ~100 nm. It can be seen that Al nanoparticles dominate in the sample, despite their lower (in comparison with iron) density. The difference in the atomic masses of iron and aluminium allows one to recognise these materials from the contrast of TEM images: iron has a higher contrast. Figure 2 shows a TEM image of an irradiated mixture of iron and aluminium colloids.

The melting temperatures of iron and aluminium are, respectively, 1530°C and 658°C. In this context, the iron nanoparticles covered by the laser beam during irradiation undergo melting later than aluminium nanoparticles during laser irradiation and pass to the solid phase earlier when the irradiation is over. It can be seen in Fig. 2 that the size of the iron core of core–shell nanoparticles is much larger than the initial size of iron nanoparticles (Fig. 1b). The inset in Fig. 2 shows that some of core–shell nanoparticles are multicore ones. An analysis of Fig. 2 makes it possible to plot size distributions of core–shell nanoparticles and their Fe cores (Fig. 3).

It can be seen in Fig. 3 that the average size of Fe core increases by a factor of about three and the distribution maximum is in the vicinity of 25 nm. At the same time, the size of core–shell Fe@Al particles is 50–80 nm, which indicates a decrease of aluminium nanoparticles in size.

Under conditions of this study, the temperature of iron nanoparticles significantly exceeds the melting temperature of bulk iron; hence, particles can coagulate with the formation of a sphere, whose diameter greatly exceeds their initial size. Note that the cubic shape of some initial iron nanoparticles [11], observed in Fig. 1b, changes to spherical after laser irradiation. Cobalt nanorods undergo a similar transformation: they acquire a spherical shape during laser heating in liquid ethanol [10]. This transformation is apparently caused by the surface tension forces, which provide a shape with minimum

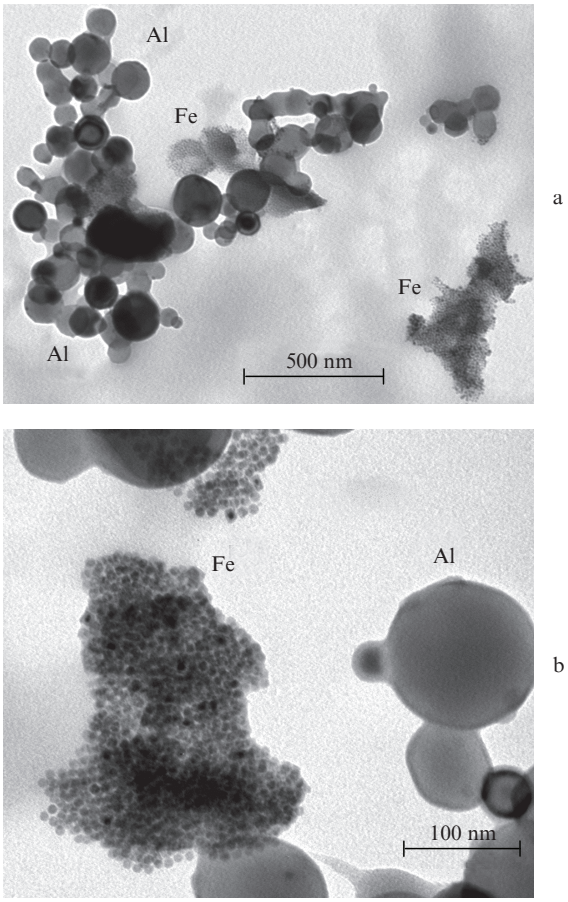

Figure 1. TEM images of the initial suspension of aluminium and iron nanoparticles in absolute ethanol.

surface energy for the melt: spherical. This shape is typical of most nanoparticles obtained by laser ablation of solids in liquids.

Under steady-state conditions, four stable phases are formed in alloys of the Fe–Al system: Fe_3Al, $FeAl_2$, Fe_2Al_5, and $FeAl_3$. Each of them has a certain homogeneity range, depending on the ratio of the aluminium and iron contents [12]. There is a region in the phase diagram of the Fe–Al pair, where both metals are liquid but do not form a stable phase.

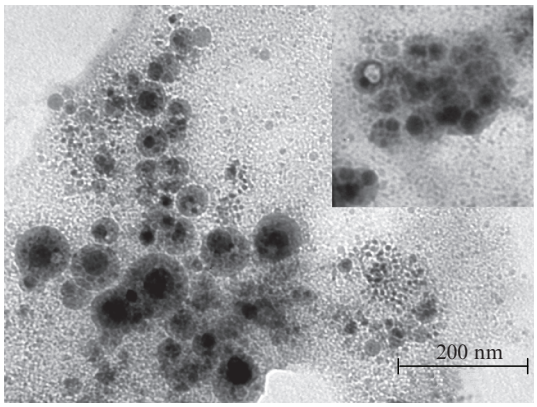

Figure 2. TEM image of the suspension of aluminium and iron nanoparticles subjected to 10-min laser irradiation at a pulse repetition rate of 10 kHz. The inset shows an enlarged image 400×400 nm in size.

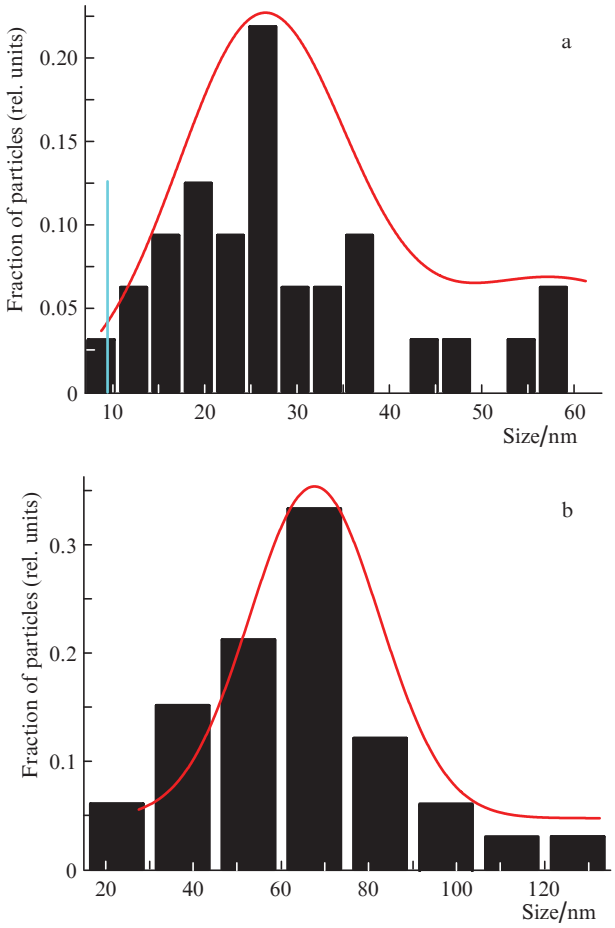

Figure 3. Size distributions of (a) cores of Fe@Al nanoparticles and (b) nanoparticles themselves. The vertical line in panel (a) indicates the initial size of iron nanoparticles. The solid curves are approximations.

Apparently, in this range of temperatures and relative Fe/Al contents, core–shell nanoparticles may arise without the formation of a homogeneous phase. However, one must remember that the Fe–Al phase diagram reported in the literature is characteristic of only equilibrium conditions. Generally, other phases can be formed in such a strongly nonequilibrium process as pulsed laser heating of nanoparticles.

Since the initial colloidal solution of the aluminium–iron mixture was obtained by adding individual powders of metals to the common dispersed medium (absolute ethanol), the core–shell Fe@Al nanoparticles, observed in Fig. 2, were formed due to the interaction between the molten components. These conditions can be implemented in two ways. First, a two-component agglomerate may just find itself in the region of laser beam waist. The environmental vapour pressure will bring particles closer to each other if they are initially in contact. Heating of the agglomerate will first lead to melting of the component with a lower melting temperature (aluminium in our case), and the molten particles will wet their 'solid' neighbours to form a shell, with a possibility of forming an alloy phase at the interface upon further heating. However, a more likely process is splitting agglomerates into small particles, because coagulation and change in the shape of iron particles is observed in experiments. At the same time, nanoparticles may interact in the liquid phase as a result of aggregation of vapour bubbles, which are formed around each heated metal particle.

The vapour shell formed around a particle in a laser beam contains vapour of the working liquid in which laser irradiation occurs. In addition, since the irradiation of nanoparticles is accompanied by the formation of plasma, the shell contains also products of liquid dissociation induced by plasma electrons. In the case of water, these products include gaseous H_2 and O_2, as well as H_2O_2 [13–15]. During laser irradiation the suspension of nanoparticles in liquid ethanol (C_2H_5OH), H_2 and O_2 are released in the initial stage. The oxygen content in the liquid decreases with an increase in the total irradiation time, because this oxygen, dissolved in the liquid, is not a product of ethanol dissociation induced by plasma electrons during optical liquid breakdown. With an increase in the laser irradiation time, only one gaseous product remains in the liquid: hydrogen (H_2); i.e., the nanoparticles have a reducing environment, which impedes oxidation of their material. The released hydrogen is dissolved well in liquid aluminium; when a nanoparticle is solidified, hydrogen remains in it in the form of a cavity, as can be seen in the inset in Fig. 2. This pattern is in good agreement with the previously observed formation of Al nanoparticles with cavities during laser ablation of an aluminium target in ethanol [16]. Obviously, the aluminium shell around the iron core of Fe@Al nanoparticles is oxidised by air oxygen when nanoparticles are transported onto the microscope grid. However, this is native oxide, whose thickness does not exceed 2–3 nm. In addition, during laser irradiation of a suspension in liquid ethanol, the latter decomposes to disordered carbon [17], which can form a shell around newly formed Fe@Al nanoparticles. This shell cannot be distinguished in TEM photographs of the samples because of its low contrast and thickness.

Extinction spectra of an irradiated mixture of iron and aluminium colloids in absolute ethanol are shown in Fig. 4. The spectra of the initial mixture have no pronounced features in the range of 200–800 nm. The reason is that the size of Al nanoparticles is about 100 nm or even more, and the plasmon resonance peak of so large metal nanoparticles can barely be observed. In addition, the nanoparticles are rapidly sedimented in liquid, giving no contribution to absorption. At the same time, the plasmon resonance peak of 10-nm Fe nanoparticles, being located near 200 nm [18], is imposed on the fundamental absorption edge of ethanol. Since the fraction of faceted nanoparticles is small, there are no other resonances, which are observed in the spectra of cubic nanoparticles and correspond to vibrations along different cube axes

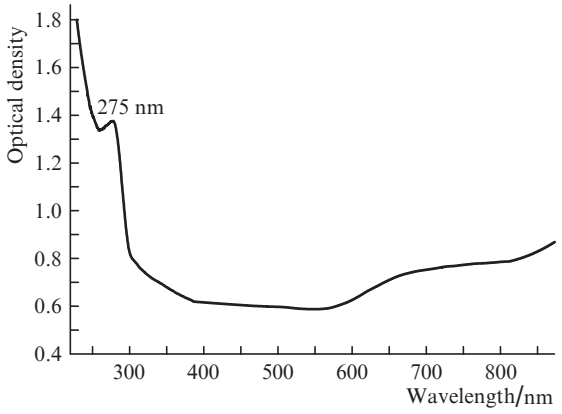

Figure 4. Extinction spectra of irradiated core–shell Fe@Al nanoparticles in ethanol.

[19, 20]. The peak in the vicinity of 275 nm can apparently be assigned to core–shell Fe@Al nanoparticles.

The core–shell Fe@Al nanoparticles obtained by laser irradiation of a mixture of colloids retain their magnetic properties. This circumstance is favourable for practical applications of these particles in medicine and in biology, because aluminium oxide Al_2O_3 is biocompatible and core–shell Fe@Al nanoparticles have magnetic properties.

4. Conclusions

It was experimentally shown that laser irradiation of a mixture of colloidal solutions of iron and aluminium nanoparticles leads to the formation of core–shell nanoparticles, whose core and shell consist of iron and aluminium, respectively. In contrast to the previous works devoted to the formation of core–shell nanoparticles, the core and shell sizes of the objects under study were found to change in opposite directions. Specifically, iron nanoparticles increase in size as a result of laser irradiation, whereas the size of aluminium nanoparticles decreases in comparison with the initial one. As in the previous studies, the formation of core–shell nanoparticles is explained by the difference in the melting temperatures of the initial mixture components. It should be emphasised that, as far as we know, the possibility of fabricating Fe@Al nanoparticles by chemical methods has not been investigated. The results obtained are indicative of flexibility of the technique of laser ablation in liquids, which makes it possible to form nanoparticles with diverse morphologies.

Acknowledgements. We are grateful to E. Anagnostopoulou and J.-L. Goffier (INSA, Toulouse, France) for their help with TEM studies.

This work was performed within State Contract No. AAAA-A18-118021390190-1 and within the framework of National Research Nuclear University 'MEPhI' (Moscow Engineering Physics Institute) Academic Excellence Project (Contract No. 02.a03.21.0005) and supported in part by the Russian Foundation for Basic Research (Grant Nos 16-02-01054_a and 18-52-70012_e_Aziya_a), Programme No. 7 of the Presidium of the Russian Academy of Sciences, and the Foundation of the President of the Russian Federation for Support of Young Russian Scientists (Grant No. MK-3606.2017.2).

References

1. Yang G.W. *Prog. Mater. Sci*., **52** (4), 648 (2007).
2. Chornya M., Fishbeina I., Yellenb B.B., et al. *Proc. Nat. Acad. Sci. USA*, **107** (18), 8346 (2010).
3. Zhang D., Gökce B., Barcikowski S. *Chem. Rev*., **117**, 3990 (2017).
4. Izgaliev A.T., Simakin A.V., Shafeev G.A. *Quantum Electron.*, **34** (1), 47 (2004) [*Kvantovaya Elektron*., **34** (1), 47 (2004)].
5. Izgaliev A.T., Simakin A.V., Shafeev G.A., Bozon-Verduraz F. *Chem. Phys. Lett*., **390**, 467 (2004).
6. Serkov A.A., Kuzmin P.G., Shafeev G.A. *Chem. Phys. Lett.*, **647**, 68 (2016).
7. Serkov A.A., Shcherbina M.E., Kuzmin P.G., Kirichenko N.A. *Appl. Surf. Sci*., **336**, 96 (2015).
8. Serkov A.A., Barmina E.V., Kuzmin P.G., Shafeev G.A. *Chem. Phys. Lett*., **623**, 93 (2015).
9. Serkov A.A., Barmina E.V., Simakin A.V., Kuzmin P.G., Voronov V.V., Shafeev G.A. *Appl. Surf. Sci*., **348**, 71 (2015).
10. Barmina E.V., Sukhov I.A., Viau G., Shafeev G.A. *Chem. Phys. Chem.*, **18**, 1069 (2017).
11. Viau G., Toneguzzo P., Pierrard A., Acher O., Fiévet F. *Scr. Mater*., **44** (8), 2263 (2001).
12. Bannykh O.A., Budberg P.B., Alisova S.P., et al. *Diagrammy sostoyaniya dvoinykh i mnogokomponentnykh sistem na osnove zheleza* (Phase Diagrams of Binary and Multicomponent Iron-Based Systems) (Moscow: Metallurgiya, 1986) p. 440.
13. Sukhov I.A., Shafeev G.A., Barmina E.V., Simakin A.V., Voronov V.V., Uvarov O.V. *Quantum Electron*., **47** (6), 533 (2017) [*Kvantovaya Elektron*., **47** (6), 533 (2017)].
14. Barmina E.V., Simakin A.V., Shafeev G.A. *Chem. Phys. Lett*., **655**, 35 (2016).
15. Barmina E.V., Gudkov S.V., Simakin A.V., Shafeev G.A. *J. Laser Micro/Nanoeng*., **12** (3), 254 (2017).
16. Stratakis E., Barberoglou M., Fotakis C., Viau G., Garcia C., Shafeev G.A. *Opt. Express*, **17** (15), 12650 (2009).
17. Sukhov I.A., Shafeev G.A., Voronov V.V., Sygletou M., Stratakis E., Fotakis C. *Appl. Surf. Sci*., **302**, 79 (2014).
18. Creighton J.A., Eadon D.G. *J. Chem. Soc. Faraday Trans*., **87** (24), 3881 (1991).
19. Kreibig U., Vollmer M. *Optical Properties of Metal Clusters* (Berlin: Springer, 1995).
20. Klimov V.V. *Nanoplazmonika* (Nanoplasmonics) (Moscow: Fizmatlit, 2009).